Feasibility study on axial pressure detection in smart rubber bearing (SRB)

Y. Zeng[(1)], P.Pan[(2)], Y.M.Guo[(3)], Y.R.Cao[(4)]

[(1)] *PhD Candidate, Tsinghua University, meishuzengyi@163.com*
[(2)] *Professor, Tsinghua University, panpeng@mail.tsinghua.edu.cn*
[(3)] *PhD Candidate, Tsinghua University, gym19@mails.tsinghua.edu.cn*
[(4)] *PhD Candidate, Tsinghua University, caoyingr2009@yeah.net*

Abstract

The base isolation system has been shown to be capable of effectively protecting structures and facilities against earthquakes. When an earthquake occurs, the rubber bearing consumes substantial energy, and is a key component of the base-isolated structure. If the rubber bearing is subjected to loads exceeding the allowable axial pressure, it may cause damage to the isolator, which results in structural failure. Therefore, it is very important to effectively monitor the axial pressure in the rubber bearings to improve the safety of the isolation structure. This paper proposes a smart rubber bearing (SRB) that can detect the axial pressure by itself. This SRB contains two active sensing layers and a conventional rubber bearing. The two active sensing layers are equipped with piezoelectric transducers and use an active sensing method to detect the axial pressure in the rubber bearing. The active sensing layer is installed above and below the rubber bearing, so the introduction of the active sensing layer does not affect the horizontal stiffness of the rubber bearing, which ensures that the SRB can easily substitute the conventional rubber bearings in engineering practice. The good potential for the axial pressure detection of the SRB was confirmed by theoretical analysis. Axial pressure detection tests were carried out on a full-scale SRB and quick-drying glue was used to bond the transducers and bearing in the SRB. A swept frequency signal from 1 kHz to 100 kHz and a white noise signal with an amplitude of 800 V were used as the detection signal. A wavelet packet-based axial pressure index is proposed to represent the axial pressure in the SRB. When the transducers were installed on the same vertical axis, both the swept frequency signal and white noise signal obviously reflected the axial pressure change in the SRB, and the axial pressure index increased almost linearly with the axial pressure. The measured signal did not reflect the change of the axial pressure in the SRB when the transducers were installed on a different vertical axis.

Keywords: Smart rubber bearing; active sensing method; piezoelectric transducer; wavelet packet based index

1. Introduction

The mitigation of seismic response of structures is one of the major challenges in structural engineering[1]. Over recent decades, the base isolation system has been shown to effectively protect structures and facilities against earthquakes[2, 3]. The laminated rubber bearing, which was first proposed in the 1970s, is widely used in buildings. When the earthquake occurs, the rubber bearing consumes a lot of energy, and it is the key and weak part of the structure. If the rubber bearing is subjected to axial loads exceeding the allowable pressure, it may cause damage to the bearing, which results in structural failure. Therefore, effectively monitoring the axial pressure in rubber bearings is important for improving the safety and reliability of base isolation structures.

Some scholars have studied the damage detection of rubber bearings. Kawasaki Y et al.[4] used acoustic emission (AE) method to evaluated the generation of micro-cracks inside the bearings. This method can successfully identify the micro-cracks and their positions inside the rubber bearing, but cannot reflect the overall performance of the rubber bearing, such as stress and deformation. Akira Mita and Yutaka Yoneda[5] used ultrasonic wave to detecte whether there are lead core inside the laminated rubber bearing. They used a quite small rubber bearing with a diameter of 100 mm and arranged the wave generator and vibration sensor on the side of the rubber bearing. It should be noted that the rubber bearings used in practical engineering are usually over 600mm in diameter, and the wave generator and vibration sensor arranged on the side is easy to fall down when the bearings sustain large shear deformation. In summary, there is currently a lack of method to detect the axial pressure of the rubber bearing.

In this study, a smart rubber bearing (SRB) is proposed, and a feasibility study of axial pressure detection in SRB was conducted. The detection principle was first demonstrated. Then a full-scale SRB with a diameter of 600 mm was used for testing, and detection tests were carried out under different axial pressures in the SRB. A wavelet packet based axial pressure index is proposed to express the axial pressure in the SRB. Finnaly, the influence of experiment setting and experment result is discussed.

2. The structure and axial pressure detection mechanism of the Smart Rubber Bearing (SRB)

2.1 The structure of the Smart Rubber Bearing(SRB)

The structure of SRB is shown in Fig.1. The SRB includes a pair of active sensing layers and a rubber bearing. The active sensing layers are placed at the top and bottom of the rubber bearing; therefore, the horizontal stiffness of the SRB is the same as that of a conventional rubber bearing. The main purpose of the active sensing layer is to protect the transducers and electric wires from being crushed. The active sensing layer comprises a steel plate, two types of bolt holes, trunkings, measuring holes, electric wires, and piezoelectric transducers. Trunkings and measuring holes are used to place electric wires and piezoelectric transducers.

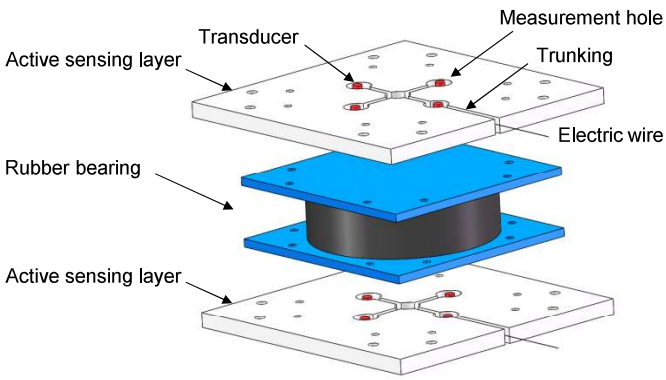

Fig.1. Structure of SRB.[6]

2.2 Axial pressure detection mechanism in the SRB

Active sensing method using stress waves is applied to detect the axial pressure change in the SRB. Fig.2 demonstrate the mechanism of axial pressure detection in the SRB. A pair of piezoelectric transducers are installed in the top and bottom active sensing layers. One is used as a wave generator to generate stress waves which propagate along the rubber bearing, and the other acts as a vibration sensor to detect the wave response. Moreover, these two transducers are approximately on the same vertical axis to ensure the quality of the measured signals. The stress wave is generated by a wave generator, passes through the rubber bearing, and is finally detected by the vibration sensor.

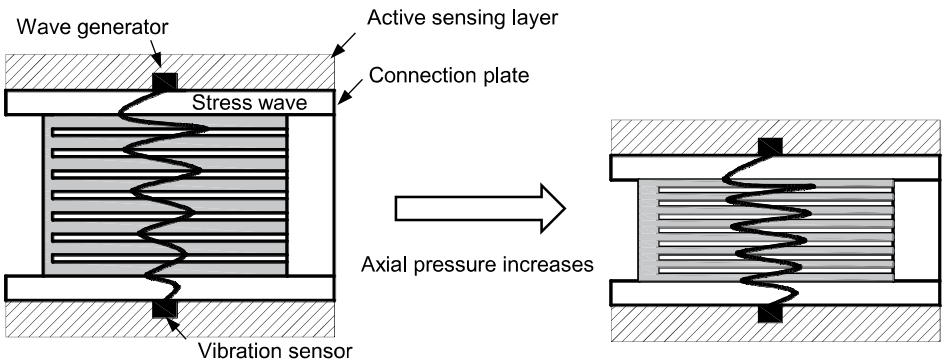

Fig.2. The mechanism of axial pressure detection.[6]

When the axial pressure of the SRB increases, the deformation of rubber increases and the thickness decreases, so the propagation path of stress wave becomes shorter and the energy loss becomes smaller. In this way, analysis of the measured signal can reveal the variation of axial pressure in the SRB.

3. Experiment setup and axial pressure index

3.1 SRB specimen

A full-scale SRB with a diameter of 600 mm was used in the detection tests. The dimension and the specimen is shown in Fig.3. The size of the active sensing layer and rubber bearing is 900mm×900mm×50mm and 700mm×700mm×230mm, respectively. Four wave generators and four vibration sensors, namely, G1-G4 and S1-S4, respectively, are arranged in the measurement holes of the active sensing layers. Wave generators are placed at the top, and vibration sensors are placed at the bottom. The transducers with same index, for example G1 and S1, are on the same vertical axis.

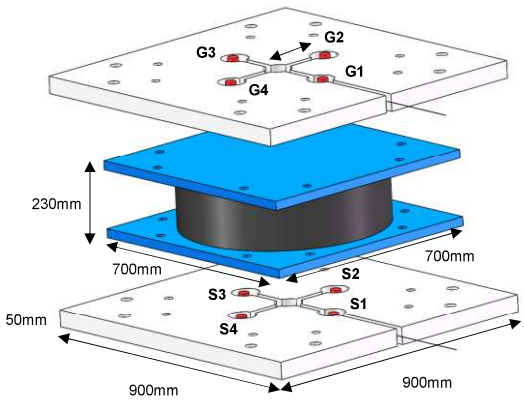

Fig.3. The dimension of the SRB specimen.[6]

3.2 Experiment setup

The experiment setup is shown in Fig.4. An electro-servo hydraulic testing machine with a loading capacity of 15,000 kN was used to load the SRB specimens. During the loading process, detection signals were generated through the NI DAQ system (NI PXle-6376) and amplified by a power amplifier (Agitek ATA-6214) to ± 400 V. After propagating in the SRB, the detection signal was measured by a vibration sensor using the same NI DAQ system at the sampling frequency of 1 MHz.

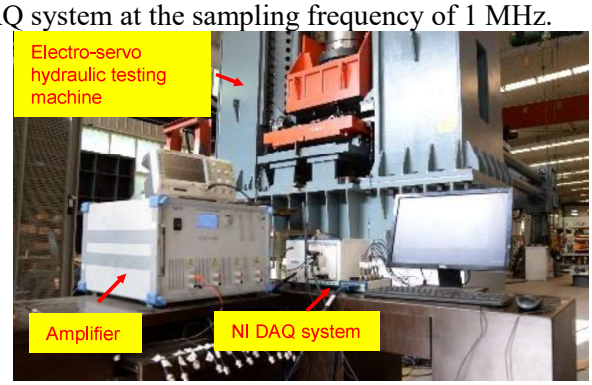

Fig.4. The experiment setup.[6]

The SRB specimen was loaded under different axial pressures. The loading scheme is shown in Fig.5. Axial compression loading starts from 0MPa and ends at 15MPa, and each stage is loaded at 2.5MPa, that is, 700kN for this SRB specimen. At the end of each loading stage, a detection signal is generated, and the vibration sensors collect the measured signal that propagated through the SRB. In order to ensure the accuracy of the experiment, the loading test repeats three times.

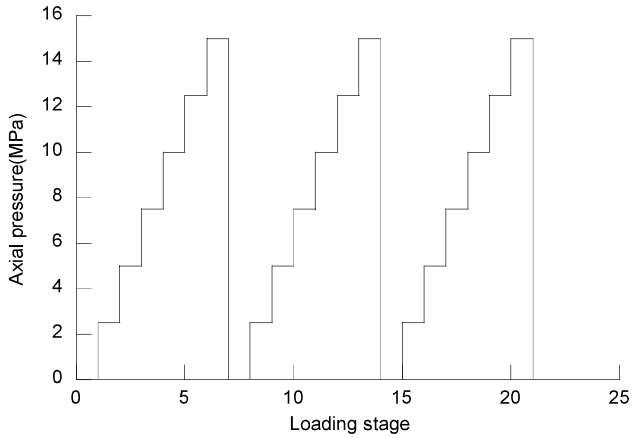

Fig.5. Loading scheme.[6]

3.3 Axial pressure index

Wavelet packet analysis is a common signal processing method, which has been widely used for damage detection in engineering structures [7, 8]. In this study, a wavelet-packet-based index was used to evaluate the axial pressure in the SRB. The procedure for establishing the axial pressure index is as follows:

Firstly, the measured signal under different axial pressure $X_i(t)$ is decomposed by into a series of subsets $x_{i,j}(t)$ with different frequency bands, where i indicates the axial pressure and j is the index of subset. Next, the energy of each subset $E_{i,j}$ is obtained.

$$E_{i,j} = \int_{-\infty}^{+\infty} \left| x_{i,j}(t) \right|^2 dt \tag{1}$$

To make the index more accurate, only specific parts of the subsets, which are sensitive to the axial pressure change, are selected to establish the axial pressure index. The selected subsets are denoted as $E_{i,k}$, where k is the index of the selected subsets.

The axial pressure index $I(i)$ is defined as follows:

$$I(i)=\frac{\sqrt{\sum_{k=k1}^{kn} E_{i,k}^2}}{\sqrt{\sum_{k=k1}^{kn} E_{1,k}^2}} \tag{2}$$

where $k1$ and kn refer to the first and last selected subset, respectively; $E_{1,k}$ is the energy of the selected subset under the axial pressure of 0 MPa

4. Result and discussion

4.1 The transmission loss of detection signal in the SRB

To investigate the transmission loss of detection signals in the SRB, tests with different arrangement of transducers are carried on. As shown in Fig.6, arrangement I is bonding the wave generator and vibration sensor directly, while arrangement II is setting the transducers in G1 and S1 as Section 3 illustrated. Since the input voltage range of the NI DAQ system is ±10 volts, in order to avoid signal of the vibration sensor exceeding the range, a swept signal with an amplitude of 20V is used in arrangement I. However, in arrangement II, due to large signal attenuation in the SRB, a swept signal with an amplitude of 800V is used.

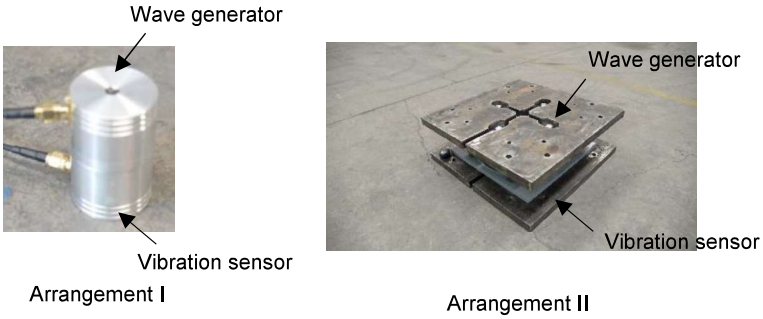

Fig.6. Two transducer arrangements.[6]

The time history of the received signal in the two arrangements is shown in Fig.7. A normalized attenuation ratio R, as shown in Eq. (3), is used to evaluate the attenuation of the signal.

$$R=\frac{Amp_{out}}{Amp_{in}}\times 100\% \tag{3}$$

Where Amp_{out} is the amplitude of measured signal, and Amp_{in} is the amplitude of input signal.

The amplitude in the arrangement I and arrangement II is 8.02V and 0.15V, respectively. The attenuation ratio in the two arrangement is 40.1% and 0.02%. The signal energy is reduced by 99.95% when the transducers are located above and below the SRB compared to the transducers bonded directly. Therefore, an amplifier which can amplify the voltage to ±400V is used in the detection of the SRB to guarantee the signal quantity.

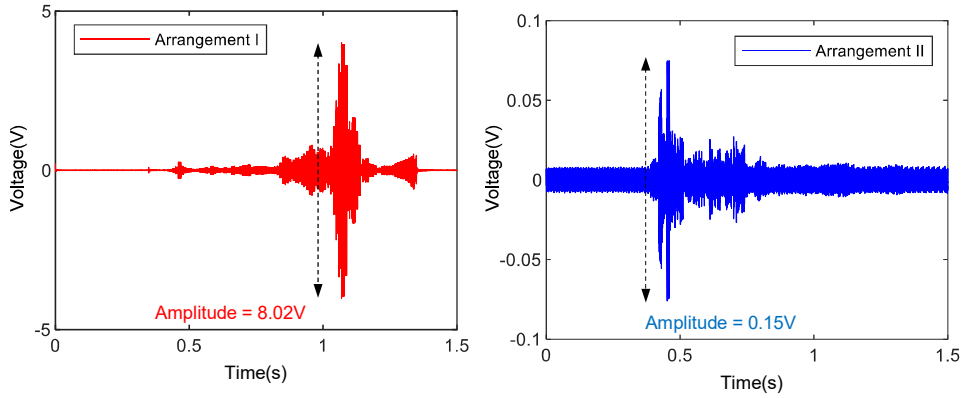

Fig.7. The time history of the received signal in the two arrangements.[6]

4.3 The comparison of different detection signal

Various types of detection signals including swept signal, pulse signal, sine signal and white noise signal are investigated before the axial pressure detection test. The time history of each detection signal is shown in Fig.8. The frequency range of swept signal is from 1kHz to 100kHz with a duration of 1s. The frequency of sine signals is 1k, 5k, 10k, 20k and 50k. The duration of the pulse signal is 20ms. The wave generator and vibration sensor is set in the G1 and V1, respectively. The signals are amplified with a power amplifier (Agitek ATA-6214) to ±400V. The measured signal is shown in Fig.9. Comparing the input signals with the measured signals, it can be found that the pulse signal has too little energy to pass through the SRB successfully. The energy of sine signals of different frequencies varies greatly, the frequency band of sine signals is too narrow and the information contained is too little. The swept signal and white noise signal contains enough energy and broad frequency band, so in the axial pressure detection test, these two signals are choosing to be the detection signals.

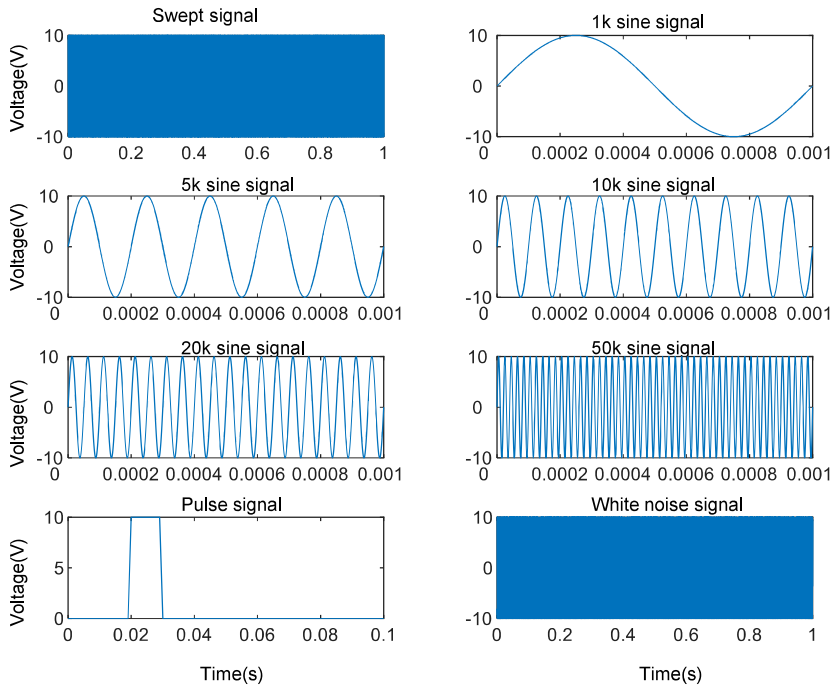

Fig.8. The time history of each detection signal.[6]

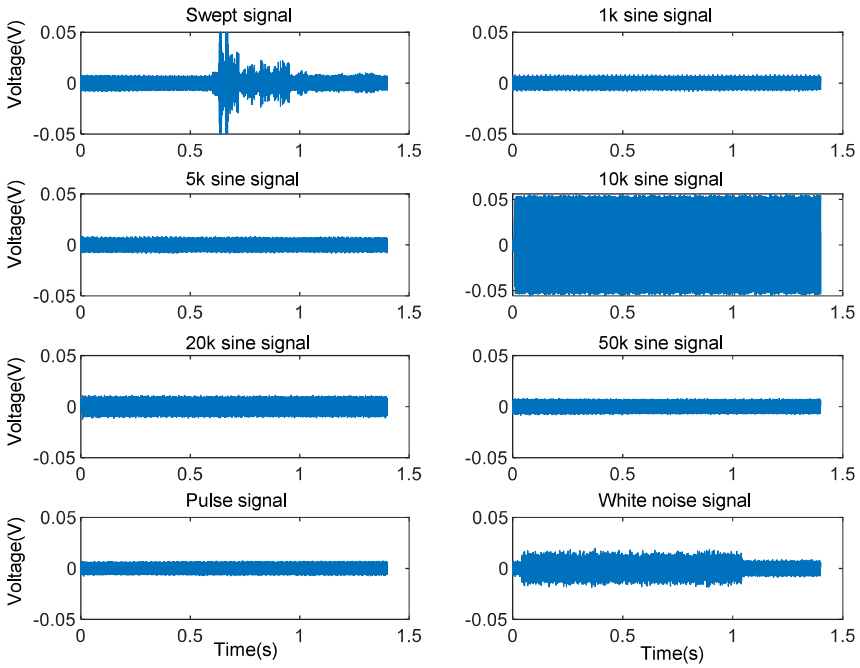

Fig.9. The time history of measured signal.[6]

4.4 The axial pressure detection in the SRB

When the wave generator is G1 and vibration sensor is S1, and the detection signal is a swept signal from 1k to 100kHz with a duration of 1s, the time history of measured signals under different axial pressure is shown in Fig.10. The time history shows that the energy of measured signal is related to the axial pressure in the SRB, but the tendency is not pronounced. Next the signals were decomposed by an 8 layers daubechie5 wavelet. After an initial analysis, it is found that the energy of measured signals mainly concentrate on the first sixteen frequency bands, so only these frequency bands are reconstructed. The wavelet packet energy spectrum of G1S1 is shown in Fig.11. G1S1 indicates the wave generator is G1 and the vibration sensor is S1. The three figures from the top to the bottom represent the first, second and third axial loading test, respectively. The x-axis is the frequency band number, while the y-axis is the energy of each frequency band. In detail, the 7 histogram in each frequency band represents the 7 stages in the process of axial loading test. As can be clearly seen from the figure, only parts of frequency bands are sensitive to the change of axial pressure. The wavelet packet spectrum is basically the same under the three axial loading tests, which indicates that the test results are repeatable and reliable. It should be noted that the result obtained in the first loading test is slightly different from that of other two loading tests. The reason is that there are some initial gaps in the SRB before the first axial loading test is carried on. After the first loading test, these gaps are compacts, thus making a small change in the measured signals.

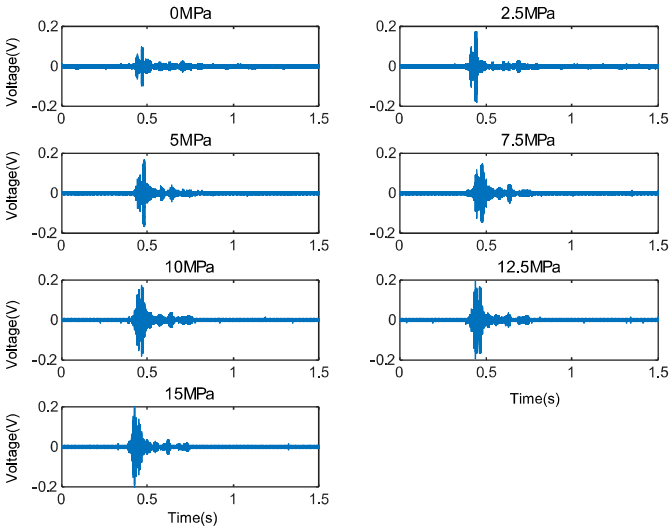

Fig.10. The time history of measured signals under different axial pressure.[6]

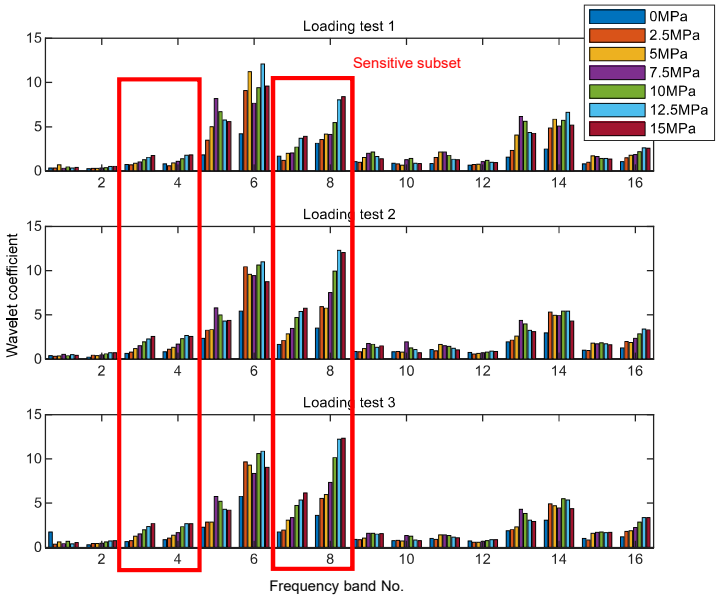

Fig.11. The wavelet packet energy spectrum of G1S1.[6]

Based on the axial pressure index proposed in Section 2.3, the axial pressure index versus the axial pressure relationship in the SRB is shown in Fig. 12. The axial pressure index increased approximately linearly with the axial pressure. However, the index suddenly changed at some points, owing to the initial defects and anisotropy of the SRB.

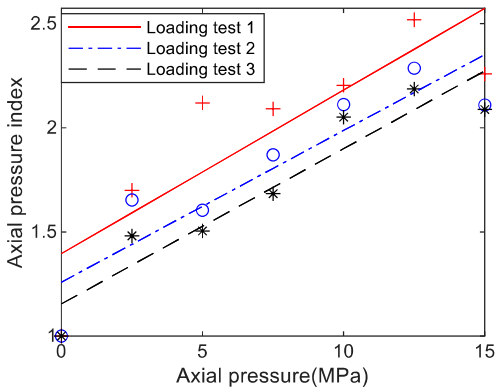

Fig.12. The axial pressure index versus the axial pressure under swept signal.[6]

When the detection signal is white noise, the axial pressure index versus axial pressure of the four arrangements is show in Fig.13. The index can also reflect the change of axial pressure in the SRB obviously. The axial pressure index under different axial pressures are fitted linearly. It shows that the swept signal and white noise signal can both reflect the axil pressure change in the SRB, and the axial pressure index increases approximately linearly with the increase of axial pressure.

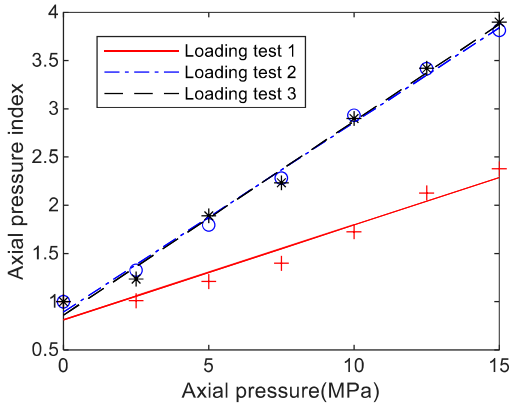

Fig.13. The axial pressure index versus the axial pressure under white noise signal.[6]

5. Conclusion

This paper proposes a Smart Rubber Bearing (SRB) comprising two active sensing layers equipped with piezoelectric transducers and a conventional rubber bearing. The good potential in the axial pressure detection of the SRB was demonstrated by theoretical analysis. A full-scale SRB with a diameter of 600 mm was used for testing. Axial pressure detection tests were carried out under different detection signals and transducer arrangements. A wavelet packet-based axial pressure index is proposed to express the axial pressure in the SRB. The main conclusions drawn from this study are as follows.

(1) The SRB contains two active sensing layers and a conventional rubber bearing. The main objective of introducing the active sensing layer is to protect the transducers and electric wires. Because the active sensing layer is installed above and below the rubber bearing, the introduction of the active sensing layer does not affect the horizontal stiffness of the rubber bearing, which ensures that the SRB can easily substitute the conventional rubber bearings in engineering practice.

(2) The axial pressure detection test results reveal that, when the transducers were on the same vertical axis, the swept frequency signal and white noise signal both reflected the axial pressure change in the SRB,

and the axial pressure index increased approximately linearly with the axial pressure. The measured signal could not reflect the change of the axial pressure in the SRB when the transducers were on different vertical axes.

Reference

1. Nakashima, M., et al., *Experiences, accomplishments, lessons, and challenges of E‐defense—Tests using world's largest shaking table.* Japan Architectural Review, 2018. **1**(1): p. 4-17.
2. Celebi, M., *Design of Seismic isolated structures: from theory to practice*. 1999: John Wiley.
3. Chimamphant, S. and K. Kasai, *Comparative response and performance of base‐isolated and fixed‐base structures.* Earthquake Engineering & Structural Dynamics, 2016. **45**(1): p. 5-27.
4. Kawasaki, Y., et al., *Health Monitoring of Rubber Bearing by using Acoustic Emission Test.* Iabse Symposium Report, 2015. **103**(2): p. -.
5. Yoneda, Y. and A. Mita, *Nondestructive inspection of a lead rubber bearing using ultrasonic wave.* Proceedings of SPIE - The International Society for Optical Engineering, 2006. **6174**.
6. Yi, Z. and P. Peng, *Feasibility study on axial pressure detection in smart rubber bearing (SRB).* Measurement, 2021: p. 109031.
7. Chen, Y.J., S.L. Xie, and X.N. Zhang, *Damage identification based on wavelet packet analysis method.* International Journal of Applied Electromagnetics and Mechanics, 2016. **52**(1-2): p. 407-414.
8. Guo, J., et al., *An experimental study on damage identification of bridge bearings based on wavelet packet analysis.* Journal of Zhejiang University of Technology, 2016. **44**(6): p. 695-698.

